

**Arsenic concentrations in shallow groundwater of Araihasar, Bangladesh:
Part I. Geological control through floodplain evolution.**

Beth Weinman^{1*}, Steven L. Goodbred, Jr.¹, Yan Zheng^{2,3}, Zahid Aziz², Ashok K. Singhi⁴,
Yogesh Chand Nagar⁴, Michael Steckler², Alexander van Geen²

¹Earth & Environmental Sciences, Vanderbilt University, Nashville, TN 37235

²Lamont-Doherty Earth Observatory of Columbia University, Palisades, NY 10964

³Queens College, City University of New York, Flushing, NY 11367

⁴Physical Research Laboratory, Navrangpura, Ahmedabad, India 380 009

*Corresponding author

Department of Earth and Environmental Sciences

Vanderbilt University

VU Station B #351805

2301 Vanderbilt Place

Nashville, TN 37235-1805

phone: 615-322-2976

fax: 615-322-2138

Submitted to Water Resources Research, January 9, 2006

Abstract

This study examines the lateral heterogeneity of shallow (<23 m) groundwater arsenic concentrations at lateral scales of 10^1 - 10^3 m in the context of floodplain morphology and evolution in Araihaazar, Bangladesh. A total of 95 auger cores and 200 shallow wells sampled over a 25 km² area indicate that the concentration of arsenic in shallow groundwater varies with the thickness and distribution of fine-grained (< 63µm) sediments that cap aquifer sands. Lower arsenic concentrations are typically found where sands outcrop at or near the surface; higher arsenic levels are observed underneath thicker fine-grained deposits. Optical luminescence, ²¹⁰Pb, and ¹³⁷Cs measurements indicate that the distribution of these deposits is not random and reflects local river history and floodplain development. A worrisome finding is that artificial raising of villages to protect them from flooding mimics the natural stratigraphy that is associated with high concentrations of arsenic in shallow groundwater.

Index Terms

1090 Field relationships (3690, 8486)

1130 Geomorphological geochronology

1803 Anthropogenic effects (4802, 4902)

1825 Geomorphology: fluvial (1625)

1831 Groundwater quality

INTRODUCTION

The occurrence of arsenic in recent alluvial aquifers of many fluvial and deltaic systems has become a well known tragedy affecting at least 100 million people in South and Southeast Asia (e.g., McArthur et al., 2004; BGS/DHPE report, 2001; Berg et al., 2001; Chen-Wuing et al., 2004). After nearly a decade of researching the mechanism(s) of the crisis, it has become increasingly evident that distinct spatial patterns in arsenic contamination exist. The Ganges-Brahmaputra and Red River delta complexes exhibit down-river enrichment trends in tube-well arsenic (BGS/DPHE, 2001; Berg et al., 2001), and other definable variance occurs in medium-to-small fluvial drainages of West Bengal and the alluvial fans of Taiwan and Inner Mongolia (Sengputa et al., 2004; Chen-Wuing et al., 2004; Smedley et al., 2003).

For the most part, such regional trends (10^1 - 10^2 km) in dissolved arsenic distribution can be explained by geological properties. In Bangladesh and West Bengal, Tertiary and Pleistocene upland deposits remain relatively unaffected by arsenic, whereas Holocene floodplains and delta plains typically have moderate (40-60% of tube-wells $>10\mu\text{g/L}$) to strong enrichments ($>80\%$ of tube-wells $>10\mu\text{g/L}$) of shallow groundwater arsenic (Ahmed et al., 2004; BGS/DPHE, 2001; Acharyya et al., 2000). Even within the frequently arsenic-rich Holocene aquifers, patterns of tube-well arsenic correspond with large-scale (10s of kilometers) geologic and geomorphic features (Yu et al., 2003). Less well studied has been the significant spatial structure and heterogeneity of arsenic at intermediate scales (2-10 km) observed in a few special study areas more densely sampled by BGS/DPHE (2001).

In this paper, we focus on geological controls of the heterogeneity of shallow (<23 m) groundwater arsenic at even finer scales of 10s to 1000s of meters. This local-scale variability in arsenic was first recognized in a comprehensive 6000 tube-well survey in the 25 km^2 'upazila' of

Araihazar, Bangladesh (van Geen et al., 2002; 2003). This area is a complex, modern distal floodplain setting, situated west of the current Meghna River and juxtaposed by two uplifted Pleistocene terraces (Fig. 1). It also occupies a location previously influenced by the Brahmaputra River prior to its westward switch ~150 years ago (Fergusson, 1863). In this particular setting, the distribution of arsenic in groundwater is extremely heterogeneous, with concentrations differing by as much as 50-fold (e.g. 7 vs. 321 $\mu\text{g/L}$) for tube-wells located only 10 m apart and screened at the same depth (van Geen et al., 2003). Variations in the concentration of groundwater arsenic at this very small scale are beyond the scope of this study, but even predictions at the scale of 100s-1000m at which villages are constructed could have significant implications for mitigation.

McArthur et al. (2004) and Horneman et al. (2004) have suggested that the nature of surficial deposits might control the distribution of arsenic in underlying shallow aquifers. This notion has been reinforced with a companion study by Aziz et al. (this volume) showing that variations in shallow-aquifer arsenic at scales <1 km within the Araihazar floodplain are significantly correlated with geophysical properties of the top ~5-6m of sediment. In the present paper, we explore the origin of this relationship in terms of floodplain evolution by first correlating 10^3 m-scale distributions of groundwater arsenic to patterns of modern and relict stream channels. We then examine whether fine-scale (10^1 - 10^2 m) patterns of groundwater arsenic are controlled by local fluvial subenvironments (e.g., crevasse splays, point bars, and levees). We also determine if anomalies in fine-scale distribution of groundwater are geologically controlled by lateral discontinuities in stratigraphy. Finally, we examine the potential effects of anthropogenic floodplain modification on arsenic concentration and aquifer ventilation. The hope is that the mechanistic understanding obtained from this investigation will

help guide arsenic mitigation through the complex geological features that characterize fluvial-deltaic sedimentary basins.

1. METHODS

To evaluate the effect of floodplain morphology on the level of arsenic in shallow groundwater, a sedimentological and stratigraphic investigation of near-surface deposits was conducted in the physically diverse floodplain of Araihasar (Fig. 1). Several previous geochemical and hydrological surveys (van Geen et al., 2002 and 2003; Horneman et al., 2004; Zheng et al, 2004 and 2005) make this area a prime location for testing the hypothesis that the heterogeneity of dissolved groundwater arsenic correlates with changes in near-surface geology. In all, four transects comprising 95 hand-auger and 15 shallow needle-sampler profiles were collected (see van Geen et al., 2004 for description of needle-sampler). Site selection was based on surface-conductivity measures (EM-31) and shallow-aquifer arsenic data (Aziz et al., this volume). Grain-size analysis was performed on 19 auger and 11 needle-sample profiles to differentiate the types of sediments that comprise the local floodplain. Based on detailed field descriptions and grain-size distributions, the data were organized into major sediment types (sedimentary facies). The stratigraphic succession of these sediment types were similarly compiled from auger and needle-sampler data, as well as field notes. Resulting stratigraphic facies were identified on the basis of sediment type, thickness, and stacking patterns. Distribution of these stratigraphic facies, along with a digital elevation model, radiometrically derived accretion rates, and luminescence dating allowed for a reconstruction of the floodplain's history. The resulting floodplain-evolution model was then compared with arsenic distributions

in ArcView-GIS using a subset of 200 tube-wells from the survey of van Geen et al. (2003) that are <15m deep and located within 50m of the auger transects.

1.1. Sediment Grain Size and Facies:

Sediment samples were collected along four transects across the study area (I-I', II-II', III-III', and IV-IV'), with augering sites nested to capture both larger-scale (10^3m) and smaller-scale (10^1m - 10^2m) variability in the distribution of shallow groundwater arsenic (Fig. 2). Of the 95 hand augers, 56 were located in low-lying cultivated fields where deposits are relatively undisturbed, as compared with many village areas where there has been significant anthropogenic reworking and build-up of local sediment. Of the remaining auger samples, 11 were from eight villages with drastically different tube-well arsenic concentrations (means ranging from 5 to $>500\mu\text{g/L}$) and 28 augers were collected next to shallow tube-wells ($<15.2\text{ m}$) with dissolved arsenic concentrations ranging from 5 to $879\mu\text{g/L}$. All augers were drilled through the surface mud cap and typically 50 cm or more into the underlying sand unit (i.e., the shallow aquifer).

The characterization and interpretation of stratigraphic facies was based on detailed field descriptions and validated by grain-size analysis of a subset of 129 samples taken from 30 auger and needle-sampling locations. Grain-size distributions were determined using a settling tube for sediment fractions greater than $63\mu\text{m}$ and a Micromeritics Sedigraph 5100 for the $<63\mu\text{m}$ fraction (Lamy et al., 1998). The organic fraction associated with each sample was determined by loss-on-ignition (LOI) at 450°C for 6 hours. A cluster analysis of the measured LOI, sand ($>63\mu\text{m}$), silt (4 - $63\mu\text{m}$), and clay ($<4\mu\text{m}$) fractions using unweighted pair-group averaging and Euclidean distancing of the variables was performed to identify the sediment facies of the recent floodplain (Clifford and Stephenson, 1975). Clustering results were consistent with field

descriptions and facies previously identified in the Bengal basin (Ahmed et al., 2004; Goodbred and Kuehl, 2000).

1.2. Sediment Accretion and Dating

Sediment accretion rates were determined using ^{137}Cs and ^{210}Pb radionuclide inventories (He and Walling, 1996; Goodbred and Kuehl, 1998) measured along a transect of about 1 km from a point-bar along the modern channel to the distal floodplain (Fig. 2). Samples of fine-grained surface sediments were collected using a 50-cm push core, drying and homogenizing 25-cm intervals, and placing a ~100 g portion from each interval in sealed containers. The activity of ^{137}Cs ($T_{1/2} = 30.17$ yr) and ^{210}Pb ($T_{1/2} = 22.3$ yr), was determined by gamma spectroscopy using a low-energy (planar) intrinsic germanium detector. Each sample was allowed to reach secular equilibrium with parent ^{226}Ra ($T_{1/2} = 1.60 \times 10^3$ yr), and self-absorption of low-energy ^{210}Pb gamma emission was corrected for (Cutshall et al., 1983). On the basis of ^{137}Cs and ^{210}Pb inventories at each site, floodplain sedimentation rates were calculated using the method described by He and Walling (1996) and Goodbred and Kuehl (1998).

Four coarse-grained sediment samples were collected from sandy deposits directly underlying the fine-grained floodplain cap (depths 65, 100, and 109cm, Table 3) or sand layers within the muddy floodplain cap (depth 35cm, Table 3) for optically stimulated luminescence dating (OSL) of quartz grains. The stratigraphic location of these samples was chosen specifically to determine the most recent time that high-energy fluvial processes were active at each site. OSL techniques measure the amount of time since a unit of sediment has been exposed to sunlight, i.e., the time lapsed since burial (Jain et al., 1999; Kale et al., 2000; Srivastava et al., 2001).

For the Araihaazar samples, quartz grains were extracted after a sequential treatment with 1N HCl and 30% H₂O₂ to remove carbonate and organic matter, respectively. Following mineral separation using sodium polytungstate (2.58 g/cc), quartz-rich grains of 90-125 μm size were selected by sieving and etched for 80 minutes in 40% HF. Luminescence measurements were made using Blue Light Stimulated Luminescence (BLSL; 470nm, ~50mW/cm²) through a U-340 and Schott BG-39 filter combination on an upgraded TL/OSL Riso TL-DA-15 automated system. External dose rate was measured using thick source ZnS (Ag) alpha counting, and gamma counting was used for potassium determination. Equilibrium in the decay chains was assumed, and the cosmic-dose-rate estimation was based on Prescott and Hutton (1988). Paleodoses were determined on 20-30 aliquots by single-aliquot regeneration (SAR protocol; Murray and Wintle 2000). Results from individual aliquots were rejected if there was a poor fit of the growth curve or if the recycling ratio fell beyond the range 1.0±0.1. Age computations were based on a weighted mean of the minimum 10% of paleodoses with a weighted mean of all the paleodoses calculated for comparison. Experimental errors may include those in paleodose measurements (photon statistics), measurement of K, U, Th, and in source standards and calibrations.

1.3. Paleotopography and Modern Floodplain Elevations

A coarse paleotopographic map of Araihaazar was constructed from widespread auger data by interpolating field measurements of depth-to-sand measurements on a 25 m × 25 m cell-sized raster using the spatial analyst in ArcViewGIS. The resulting paleo-surface was then projected over IRS-1D Panchromatic and Ikonos imagery (Fig. 2). This paleo-sand surface was not corrected relative to the modern elevation difference in Araihaazar due to the limited number of auger locations.

Modern floodplain elevation data was used for four coring transects (I-I', II-II', III-III', and IV-IV', Fig. 2) to reconstruct cross-sectional stratigraphies. The relative vertical position of stratigraphic facies were adjusted according to Shuttle Radar Topography Mission (SRTM) digital terrain elevation data (DTED) and interpolated into cross-sectional profiles for paleotopographic interpretation. The SRTM DTED Level 1 data comprises elevations at 90-m post spacings, a suitable resolution for distinguishing differences in geomorphology over spatial scales of 100-1000 m.

2. RESULTS

2.1. Sedimentary Facies

Four major sediment facies (facies *i*, *ii*, *iii*, *iv*), defined mostly by the percentage of silt in the sediment and gradual fining of other components, dominate the surficial floodplain of Araihasar (Fig. 3). These facies include: (*i*) a well-sorted sand with ~85-100% of the particles in the 100-500 μm size range and very little silt; (*ii*) a moderately well-sorted silty to fine sand with > 50% of the grains 63-250 μm , which locally grades to (*ii_a*) a clean, coarse silt; (*iii*) a poorly sorted assemblage with a 2:1 ratio of silt to clay and a significant component of very-fine sand, which locally decreases to (*iii_a*) <10%; and (*iv*) a clay-rich unit with >50% content of particles <4 μm in size (Table 1). These classifications are similar to lithofacies recognized by Ahmed et al. (2004) and are typical of the silt-dominated sediment load of the Ganges and Brahmaputra rivers with variable admixtures of bedload (sand) and washload (clay) material (Datta and Subramanian, 1997).

2.2. Stratigraphic Facies

Five distinct stratigraphic facies (facies *A*, *B*, *C*, *D*, *E*) are identified on the basis of field observations of the thickness and stacking order of the sedimentary facies (Fig. 4 and Table 2). Clean sands of the shallow aquifer (i.e. facies *i*) comprise the lower unit of each sequence; the stratigraphic successions are differentiated by the thickness and texture of the overlying sediments. The primary sequences include shallow-aquifer sands that: (*A*) outcrop at the floodplain surface or are capped by (*B*) alternating decimeter-scale beds of silt and sand; (*C*) a variably thick mud unit; (*D*) a thick (>3m) clay-rich mud unit; or (*E*) highly variable, though generally muddy, anthropogenic fill.

Facies *A*, where the shallow-aquifer sands outcrop or are covered by <20 cm of finer material, is widely distributed as curvilinear or oblate features that are topographically elevated 1-3 m above adjacent floodplains (Table 2). Facies *C* is similar to *A*, except that it is bound at the surface by a fine silt, mud, or clay sequence from 0.5 to ~3 m in thickness. Facies *C* is also widely distributed, occurring throughout the study area as broad, flat plains that are typically cultivated for rice. Unlike the extensive coverage of stratigraphic facies *A* and *C*, the alternating sand/silt sequence of facies *B* is largely restricted to the edges of facies *A*, where it appears to be transitional with the lower-lying facies *C* sequence. The alternating sand/silt bedding of facies *B* displays successive units (~20-50cm thick) of coarse silts and fine sands with cm-scale tabular and trough cross-bedding structures. Facies *D* is interspersed throughout Araihasar and reflects sites where shallow fine-grained sediments are several meters thick, locally up to 10 m (facies *D*). As in the other stratigraphic facies, the surface mud unit overlies clean sands, but in facies *D* it is distinguished by its much greater thickness and generally finer grain size (facies *iv*, *iv_a*). The

distribution of facies *D* is largely restricted to several low-lying, northeast-southwest trending depressions that remain wet throughout the year.

Finally, stratigraphic facies *E* is a common succession within the villages, where the majority of tube-wells are located. Facies *E* is typified by 0.5-3 m of muddy anthropogenic fill that has been placed on top of a previously natural sand stratigraphy (i.e., facies *A*) to provide elevation above flood levels. It appears that the fill most often comprises the muddy surface unit of facies *B* and *C* that has been reworked from the adjacent floodplain. The anthropogenic origin of these units is evidenced by its content of brick, pottery, and garbage, and corroborated by statements from local landowners.

2.3. Geomorphology and Paleotopography

Comparisons with field observations show that the Ikonos and DTED data reflect actual elevation differences within Araihasar. Map views combined with DTED data show that villages (i.e., tree-covered areas with high density of tube-well data) usually conform to the elevated portions (~10m) of the fluvial topography, while neighboring fields and streambeds lie at lower elevations (~3-7m). Although the absolute elevation based on DTED data can be influenced by tree cover, the higher elevation of the villages holds even where we were able to correct for the height of trees based on differential GPS measurements. To limit the impact of flooding, villages are indeed built at naturally elevated sites or on land artificially raised by filling.

Geological cross-sections were reconstructed by combining sediment-facies data with DTED-derived elevations to illustrate the distribution of stratigraphic units within the floodplain and shallow-aquifer (Fig. 5). The cross-sections reveal that fine-grained strata of silts and clays (facies *B*, *C*, and *D*) grade together to form a widespread drape of muds over shallow aquifer

sands, which can locally outcrop to form stratigraphic facies *A*. The fine draping of muds vary in thickness from ~0-10 meters, with the finest sediments restricted to the upper several meters of the floodplain (Figs. 2 and 5). Lower-elevation areas typically comprise the finer strata of facies *C* and *D*, with the latter at locations where silt layers are up to 10 m thick. Strikingly, such fine-grained silt layers are observed outside low-lying areas only where they have been used to raise villages and contribute to facies *E*, which resembles the naturally formed facies *C* and *D*. Finally, facies *B* is found locally at the transition from low floodplain environs (facies *C* and *D*) to sandier areas of natural elevation (facies *A*).

Topographically, the base of the fine-grained surface layer defines a paleo-surface of sands within Araihaazar (i.e., the sand surface stripped of mud). Such backstripping reveals sandy deposits of higher and lower elevations, which is useful for identifying relict channel, bar, and levee features (i.e., facies *A* and *B*). The slope of this paleo-sand-surface varies from ~0.1-9°, with the steeper slopes coinciding with transitions between stratigraphic facies (i.e., facies *B*). When this surface is normalized to patterns in local elevation, the undulatory nature of the boundary is typically preserved. This is also the case for villages built on anthropogenic fill of stratigraphic (facies *E*), indicating that the sites were already naturally elevated above the floodplain before being modified by humans. In regions where they overlap, topographies obtained independently from differential GPS and DTED both indicate shoaling of the paleosand surface underneath these villages. This indicates that clusters of trees within villages do not dominate the DTED observations.

2.4. Evolution of the Floodplain

Inventories of unsupported ^{210}Pb exceed atmospheric input (25.3 dpm/cm^2 , Goodbred and Kuehl, 1998) only at two sites inside the western meander of the Old Brahmaputra River; inventories at all locations show little active accumulation (Table 5 and Fig. 2). This indicates that recent (<100 yrs) fluvial sediment input has been limited and spatially localized in Araihaazar. The inference of low sedimentation during the past century is supported by very low non-atmospheric ^{137}Cs inventories (Table 5). The accretion rates derived from ^{210}Pb and ^{137}Cs average 0.05 ± 0.06 and 0.06 ± 0.08 cm/yr, respectively. There are minor discrepancies between ^{137}Cs and ^{210}Pb -derived accretion rates at certain sites, but this is not unexpected given the different input histories for these nuclides as well as the complexity of floodplain sedimentation patterns (He and Walling, 1996; Aalto et al., 2003). The results agree well with accretion rates typical of distal floodplain environments (~ 0.10 cm/yr; Goodbred and Kuehl, 1998) and indicate that the Araihaazar floodplains are effectively relict and have received no significant sediment input within the past century.

Long-term accretion rates derived from the OSL ages are also comparable to those determined from ^{210}Pb and ^{137}Cs , with an average rate of 0.12 ± 0.03 cm/yr. Luminescence dating of the paleo-sand surface at two sites close to the modern stream (OSL1, OSL2; Figs. 2, 4; Tables 3, 4) indicates burial of the aquifer sands beginning approximately 600 years ago. This transition from clean, cross-bedded sands to fine-grained overbank muds indicates decreased fluvial energy and the beginning of abandonment by the main river channel. Sand beds (<15 cm thick) reappear locally within the muddy floodplain cap, and at site OSL1 yielded an age of ~ 400 years ago, presumably because of a temporary reactivation or a large flood of the channel around this time. In contrast to these two sites, both of which lie along the large channel feature in the

north, the age of the shallowest (i.e., youngest) sand layer at OSL3 in the meandering scroll plain of northeast Araihasar yields a considerably older age of 1000 years. This sand layer is relatively minor (i.e., <5 cm thick and mixed with muds) and is at least 1 m shallower than the underlying aquifer sands, implying that the meandering channel was probably abandoned more than 1000 years ago.

2.5. Distributions of Arsenic within the Floodplain

The subset of 200 shallow wells in the area that are located within 50 m of the auger transects indicate that arsenic concentrations in the shallow groundwater are broadly related to local geomorphology and shallow stratigraphy. The highest arsenic concentrations are typically associated with thick mud strata (facies *D*) and both natural (facies *C*) and anthropogenic (facies *E*) mud-capped sands. Similarly, areas of lower arsenic concentration are commonly associated with sandy stratigraphy that outcrops at or near the surface (facies *A* and *B*, respectively) (Fig. 5a-d). Aside from these general associations, patterns at the scale of 10s of meters show further complexity (see Figure 5). Even within villages with relatively high or low levels of arsenic in tube-wells, there often are a few wells with very different arsenic concentrations. In this paper, however, we focus on the major trends occurring at spatial scales of 100s of meters because this is the characteristic scale over which floodplain stratigraphy varies.

2.5.1 Transect I-I': This transect obliquely follows the major NE-SW trending fluvial system in Araihasar, crossing many of its geomorphic features, including levees, channel bars, and infilled channels (Fig. 2). The OSL dates suggest that the river which deposited the shallow-aquifer sands in this area existed until ~600 years ago, after which the system was progressively abandoned. Along the eastern end of transect I-I' (i.e., at a transect distance of 5400-6300 m), sands outcrop (facies *A*) or are shallowly buried (facies *B*) in association with relict bar and levee

features. Arsenic concentrations in shallow groundwater of this area are generally low, particularly when compared to areas further west (towards I). Along western portions of the transect, the capping of clayey silts thickens in low-lying floodplain and lower-lying abandoned channels (Fig. 5a; facies *C* and *D*, respectively). Groundwater arsenic values are generally high in such mud-capped areas, except in a relatively narrow region where sands locally reach the surface (3000-3100 m). In two portions of the transect (3600-4200 m and ~5100 m), the local stratigraphy has been modified by human dumping of fine-grained sediment to increase village elevation. As illustrated here, this modified stratigraphy (facies *E*) is commonly associated with high levels of arsenic in shallow groundwater.

2.5.2 Transect II-II': This transect (Figure 5b) traces a topography similar to that of Transect I-I', but further south, and crosscuts the more meandering channel system that is over 1000 years old. Again, enrichments in shallow groundwater arsenic correspond to sections of thicker mud-capped sands, notably in the village at ~3000-3300 m that has been artificially capped with muds (facies *E*).

2.5.3 Transect III-III': This transect is perpendicular to the two previous transects and reveals broadly similar patterns (Figure 5c), with high dissolved arsenic below the anthropogenically filled village area (~2700 m) and relatively low arsenic concentrations below unmodified, sand-dominated stratigraphy (facies *A* and *B* at ~1200 m). As in transect I-I, clusters of wells low in arsenic reflect a broader village-scale pattern, with similar low concentrations and sandy stratigraphy extending beyond the data presented in the transect. Unlike the other transects, however, transect III-III' includes some of the most contrasting sediment lithologies over short distances within Araihasar, both natural and anthropogenic. In terms of natural floodplain stratigraphy, among the thickest examples of muddy channel fill

observed in Araihasar (facies *D*; ~1500 m) is juxtaposed with a sandy levee more than 6 m higher in elevation (facies *A*; ~1800 m). The tube-well arsenic values from this area (at ~1800 m) are very high ($>100 \mu\text{g/L}$), which differs from the general association of low arsenic near facies *A*. Presumably, local-scale processes (10^1 m) play an important role where floodplain stratigraphy is strongly heterogeneous. An example of heterogeneous stratigraphy associated with anthropogenic activity is found in the village at 2400-2700 m (facies *E*). The site is capped by some of the finest-grained sediments (facies *iv_a*) in Araihasar, although field observations indicate that they are patchily distributed (this patchiness is not expressed in Fig. 5c due to the large scale). Again, the spatial heterogeneity of the stratigraphy appears to be reflected in shallow-aquifer arsenic concentrations, with a mixture of clean and contaminated wells found between 2400-2700 m.

2.5.4 Transect IV-IV': This transect also crosses the older meandering channel system and is characterized by a largely continuous and natural cap of floodplain deposits and infilled channels. High groundwater arsenic in the shallow aquifer once again underlie areas of thick fine-grained sediment cappings as seen between 300-2700 m. In immediately adjacent areas (~100 and 3300 m), arsenic concentrations drop considerably in conjunction with a more sand-dominated shallow stratigraphy (facies *A*, *B*), providing a notable contrast.

2.6 Regression Analysis

The qualitative linkages described above were more quantitatively evaluated by plotting arsenic concentration as a function of minimum, mean, and maximum depth-to-sand measurements determined using the zonal statistics spatial analyst function of ArcView 8.3 (Fig. 6). The depth-to-sand values were taken from the paleo-sand-surface interpolation in Figure 2, and for each well, the program overlies the two data sets to return the minimum, mean, and

maximum depth-to-sand values for each value of arsenic in tube-wells between 6-15 m deep. Since the auger and needle sampling locations are spatially limited, the results of the comparison are not, at this point, predictive. The results, however, do display the general trend of increasing arsenic with the thickness of the mud layer, which is what we observed in the field and in our stratigraphic transects. Though relatively weak, the correlation between arsenic concentrations and minimum depth-to-sand values support our qualitative findings ($R^2 = 0.33$; $p < 0.01$; Fig. 6a). The relationship weakens slightly when mean depth-to-sand is considered instead (Fig. 6b), and effectively disappears when considering maximum depth-to-sand (Fig. 6c). This may be because areas with thicker mud units are less likely to be tapped for tube-wells, although there may be other reasons. The better fit with minimum depth-to-sand values might indicate that arsenic concentrations are more closely linked with a tube-well's proximity to shallow or outcropping sands as compared with its proximity to a thick mud sequence.

3. DISCUSSION

3.1. Fluvial Geomorphology and Patterns of Shallow Groundwater Arsenic

Although the thickness and distribution of near-surface muds are heterogeneous, these patterns are not random and can largely be defined within traditional fluvial geomorphic classifications. A geomorphic reconstruction of the Araihasar area (Fig. 7) integrates the data from more than 100 hand-drilled augers and needle samples, over 75 km of EM conductivity coverage (Aziz et al., this volume), luminescence dating, and planform analysis of satellite images. The resulting patterns delineate features of a formerly braided, large river system, including bars, levees, and infilled channels. The braided-channel system is also seen to crosscut the meander bends of at least two older, more sinuous fluvial systems, each of which comprise a

complex of low-lying levees, infilled channels, and scroll bars (Fig. 7). Each of these river planforms are common in Bangladesh (Rasid, 1966; Coleman, 1969).

The distribution of tube-wells in this complex setting (i.e., as they indicate sites of homes and villages) naturally align elevated geomorphic features, such as bars and levees, where seasonal flooding is less frequent. This is shown in the overlay of groundwater arsenic concentrations from shallow tube-wells <22.5 m (75 ft) on the geomorphic interpretation (Fig. 7). Tube-wells associated with individual geomorphic features generally support either high or low arsenic values, or at the least large clusters of similarly contaminated wells. Hereonin, we focus on placing these general trends in a more predictable and definable context of floodplain geomorphology.

3.1.1 Channel Bars

Reviewing the association of arsenic and geomorphic features, probably the most consistent low arsenic values occur on channel bars within the former braided channel system (Fig. 7). These areas typically comprise stratigraphic facies *A* and *B*, with shallow aquifer sands lying at or near the surface. The reason for their relatively high elevation and sandy stratigraphy is that the bars develop during seasonally high river stage and flow regime (Bridge, 1993). This occurs during the summer monsoon when discharge is about 10 times greater than the dry-season (Coleman, 1969). Luminescence ages indicate that progressive abandonment of this high-energy braided channel began after 600 years ago. This probably continued until about 100 years ago when the main Brahmaputra finally avulsed to its modern course far from Arai hazar (Fergusson, 1893). The waning of discharge associated with abandonment would have led to a comparative decrease in seasonal flood height and flow velocity (Bristow, 1999). Such lower flow regimes would have favored the widespread capping and infilling of the sandy braided-channel

topography with fine-grained sediments. Locally elevated areas, such as the channel bars, would infrequently flood and thus still exposed at or near the floodplain surface. Consequently, villages became settled on these sandy elevated areas and today yield shallow groundwaters relatively low in arsenic compared with adjacent, muddier areas.

3.1.2 Levees

River levees are also common sites for human settlement, as can be seen by the elongate, curvilinear arrangement of tube-wells in many areas (Fig. 7). Again, this settlement pattern arises partly because of the levees' relatively high elevation and due to their proximity to water channels for transportation. However, in contrast with the relative homogeneity of tube-well arsenic on the channel bars, arsenic in wells associated with the levees differs considerably between the individual features. For example, some levees support almost exclusively contaminated wells, whereas others yield mostly clean shallow groundwater (Fig 7). Consistent with our observations, the main sedimentological difference in levees with high or low groundwater arsenic is the thickness and extent of the surface mud cap. In low-arsenic levees, shallow aquifer sands lie exposed at or near the floodplain surface (facies *A*); levees with contaminated groundwaters are almost exclusively those with thick mud caps (facies *C*, *E*).

What, then, is the geomorphic difference between these two types of levees? It appears that the more contaminated, mud-capped levees are largely found along the older, meandering scrollplain region in northeast Araihasar, reflecting development in a relatively low-energy fluvial regime. In contrast, the sandier, less contaminated levees are located mainly in the former braided-channel region and consequently developed under higher-energy flow regimes. The most prominent low-arsenic levee is that which forms the southern boundary of the former braided stream channel. More contaminated levees are associated with the laterally migrating

meanders of a sinuous stream (as indicated by the black arrows; Fig. 7). Because these levees were formed under a lower energy regime, they are consequently finer-grained and are at lower elevation.

The latter point gives rise to another major factor that we believe may exacerbate arsenic contamination. Apparently because many levees, particularly those lower in elevation, flood with some frequency, many have been anthropogenically modified by filling the surface with fine-grained sediment to increase elevation (facies *E*). This artificial capping of levee environments was repeatedly observed during field work by the presence of anthropogenic debris in surficial deposits. The modifications can also be recognized from our shallow geologic cross-sections (e.g., Fig. 5b, 3150 m; Fig. 5c, 2700 m). Thus, we find that human modification of the floodplain may act as a significant 'geological' agent that leads to a mud-capped stratigraphy mimicking natural conditions associated with high arsenic levels in shallow groundwater of Araihasar.

3.1.3 Scroll Bars

Scroll bars are low-lying, sandy ridges formed along the inner edges of river meanders. The scrolls actually originate as the point bars of an active meander loop, but ultimately evolve into a plain of scroll bars as the meander migrates laterally toward its outer edge and abandons the active point bar (Hickin, 1974). Several sandy scroll-bar complexes are found in Araihasar along the inner edges of the older meandering channels (Fig. 7). The natural scroll bar features in Araihasar appear to be relatively low lying, perhaps only 1-2 meters above the adjacent floodplain. However, in many circumstances the scrolls appear to have been modified with anthropogenic fill, thereby increasing their elevation and thickness of the mud cap. The general

pattern of groundwater arsenic distribution along the scroll bars is similar to that of the levees, where certain clusters of wells (over 100s m) are either largely clean or largely contaminated.

3.1.4 Floodplain Evolution

The progressive impact of the different river stages on the morphology of Arai hazar, and therefore on the arsenic content of shallow groundwater, can be summarized schematically (Fig. 8). The initial stage considers a large active braided river system, similar to that of the modern Brahmaputra, that is kilometers wide with multiple channels and bars (Coleman, 1969). Bristow (1987) describes how migration of the braided Brahmaputra channel planates the preexisting floodplain surface, replacing eroded sediments with almost exclusively channel sands and sandy bar deposits. Based on close proximity of the paleo-Brahmaputra channel before 200 years ago, we infer that the largely contiguous shallow-aquifer sands of present-day Arai hazar were deposited in a similar manner. Ultimately, river avulsion is initiated and results in progressive abandonment of the active channel, which may take place over many decades (Fergusson, 1863). Because avulsion often occurs over long time periods in the Bengal basin, the river planform actually adjusts to declining flow by switching from a braided to a meandering system (Bristow, 1999). Based upon the depositional ages of sediments, we know that this abandonment began after 600 years ago. With waning flow conditions, the large channels and interbar depressions begin infilling with fine-grained sediment. This process continued until most of the topography is infilled or the area no longer receives sediment (c.f., Rasid, 1966). Accretion rates for Arai hazar and the relatively flat topography suggest that most of the area infilled prior to complete abandonment. We presume that fine-grained sediment accretion was relatively rapid (> 0.20 cm/yr) until about 100 years ago when the main course of the Brahmaputra switched to its present course west of the Madhupur Terrace (Fergusson, 1863). This final 'moribund' stage

would be appropriate for human settlement with exposed sandy high grounds as village sites and muddy floodplains for agriculture. Indeed, residents of Araihasar report that a 'big' river occupied the area until at least 100 years ago.

3.2. Possible Mechanisms for Shallow-geological Controls on Groundwater Arsenic

In spite of the general associations discussed here, it is important to note that arsenic heterogeneities between tube-wells only meters apart is often not explainable in context of floodplain geomorphology. Field tests by augering between closely spaced (<10 m) tube-wells with contrasting arsenic concentrations commonly revealed similar stratigraphies within the top ~5m of sediment, suggesting that other factors control arsenic heterogeneity at this scale. Faulty tube-well construction has been cited as at least one mechanism responsible for such fine-scale chemical heterogeneity (Ravenscroft and McArthur, 2004; Cheng et al., 2005). Chemical stratification and vertical arsenic gradients on the order of 10s to 100s of $\mu\text{g/L}$ per meter depth in the aquifer has been cited as another (McArthur, 2004). On the other hand, such a degree of vertical heterogeneity was not observed when profiles obtained with the needle-sampler from a very narrow depth range were compared with samples from a wider depth range collected from nearby nest of monitoring wells (van Geen et al., 2004). Given the high frequency of anomalous arsenic values at any given site (van Geen et al., 2003), it seems likely that several factors may be involved.

What might be some of the plausible controls of floodplain stratigraphy on arsenic concentrations? As evidenced from the correlation between arsenic and the geophysical conductivity of sediments in the upper few meters of Araihasar's floodplain (Aziz et al, this volume), sediment grain size is a factor with potential use in predicting the distribution of arsenic in shallow aquifers. Villages with elevated levels of shallow tube-well arsenic are typically

proximal to fine-grained surficial sediments, whereas areas with lower tube-well arsenic lie closer to coarser, less electromagnetically conductive sediments. One reason for the different arsenic bearing capacities between these villages can be attributed to the ways in which grain size impacts chemical and physical processes that control arsenic reaction and transport within the aquifer. In Araihasar, arsenic in shallow-aquifer sediments is thought to be mobilized from a leachable fraction that is associated with redox-sensitive, epigenetic Fe-oxyhydroxide coatings on the aquifer particles (Horneman et al., 2004; Zheng et al., 2005). The arsenic associated with these iron coatings is thought to be mobilized under reducing conditions (BGS/DPHE 2001), with less arsenic accumulating in areas with coarser-grained stratigraphies. Finer stratigraphies in the wet, topographic lows and agricultural ploughpans favor reducing porewater conditions (Brammer, 1996), which could therefore enhance the amount of arsenic in the aquifer.

The main feature of the integrated set of observations, however, is that peaks in shallow groundwater arsenic correspond to areas overlain by, or sometimes near to, thick surficial deposits of silt and clay. Locations where arsenic levels diminish are typically characterized by coarser sediments proximal to the ground surface. We therefore suggest that such surface to near-surface exposures of shallow-aquifer sand locally enhances rates of groundwater recharge, thereby flushing dissolved arsenic and/or oxidizing it to a more immobile phase. The connection has recently been substantiated by tritium-helium dating of groundwater with the Araihasar study area (Stute et al., in revision). The fact that these recharge-capable sands occur in typically elevated portions of the floodplain — as in the case of natural levees and bars — is not insignificant, since the additional elevation sets up a higher hydraulic head. Even in the absence of significant recharge, the greater potentiometric surface of the elevated sands limits flow into

these areas from the low-lying, fine-grained settings that frequently have higher levels of dissolved arsenic.

By the same token, finer sediments could potentially enhance arsenic mobilization by retarding water flow and increasing groundwater residence time (Stute et al, in revision). This is attributable to the reduction in hydraulic conductivity associated with decreasing grain size. An order-of-magnitude comparison of floodplain transmissivity can be made using the Hazen approximation, $K = C(d_{10})^2$, whereby the hydraulic conductivity of the sediment, K (m/s), is equal to a proportionality coefficient, C (65), multiplied by the effective particle diameter such that 10% of the distribution is finer than the square of this diameter, (d_{10}). An equivalent vertical conductivity for the upper 15 m of sediment can be calculated using the harmonic mean of the samples, $K_z = 15/(\sum_i^n b_i/K_i)$, where b_i and K_i are the thickness (m) and conductivity (m/s) of the sublayer, respectively (Ingbritsen and Sanford, 1998). The range of vertical conductivities from millimeters to meters per day ($\sim 10^{-5}$ to 10^{-9} m/s) is comparable to the typical K value calculated for the silty floodplains in the region of Araihasar (0.4 m/d; BGS/DPHE 2001). Without considering horizontal flow, the corresponding transport time of groundwater to a depth of 15 m would vary between 17 days and 47 years, which comparable to the measurements by $^3\text{He}/^3\text{H}$ (Stute et al., in revision). Considering also variations in sedimentary structure, anisotropy, and horizontal flow into this conceptualization, the spectrum of groundwater transit time within the surface could be considerably larger than our range of estimates. Given that available arsenic in the aquifer appears to be easily mobilized (Zheng et al., 2005), the influence of sedimentary architecture could explain why increased concentrations of tube-well arsenic coincide with aquifers covered by thicker units of muds. Areas overlain by finer sequences experience a retardation in recharge, which in turn inhibits oxidation, and drives the local system towards a

more reducing state capable of arsenic mobilization into the shallow-aquifer groundwaters (Fig. 8).

4. CONCLUSIONS

This study demonstrates that floodplain evolution can explain much of the heterogeneity of arsenic in the shallow aquifer of Araihasar. Depositional features formed under high-energy braided-channel conditions, including levees and bars, typically have the highest natural elevation and comprise permeable sands from the ground surface to depths typical of the shallow aquifer (15-25 m). Such environments are those most commonly associated with low arsenic concentrations in groundwater extracted from tube-wells. Other levee features formed under the lower-energy conditions of a meandering system are lower in elevation and comprise finer sediments in the upper few meters of stratigraphy. Tube-wells located on meandering-stream levees are typically associated with higher groundwater arsenic, which is evidently linked with a thicker and finer-grained floodplain cap (see also Aziz et al., this volume). The relationships between arsenic in shallow and near-surface geology and geomorphology indicate a level of predictability that is relevant at the village scale. The apparent relationship between human modification of the floodplain and high arsenic levels needs further investigation. Whereas no direct relationship is established here, anthropogenic activities around village tube-wells can be extensive and result in meters of fine-grained fill capping the natural stratigraphy. Such areas typically support high concentrations of arsenic and mimic the type of floodplain stratigraphy associated with high groundwater arsenic.

ACKNOWLEDGMENTS

The authors would like to thank Uttam Karmaker, Ashraf Seddique, and Mohammed Hoque from the University of Dhaka's Geology Department and Penny Youngs from Stony Brook University's Marine Sciences Research Center for their help in the field. We would also like to thank Stony Brook University's Bob Aller and Teng-fong Wong along with Lamont Doherty's Allan Horneman, Martin Stute, and Zhongqi Cheng for their help, insight, and comments on the work presented in this paper, as well as Chris Small and the University of Texas Department of Geological Science's John M. Sharp, Jr., for their help in digitally and schematically mapping the floodplain. We also like to acknowledge David Amiel and David Hirschberg from Stony Brook University for help with radiometric analyses. Funding was provided by NSF award HYD-0229600 to Goodbred. This paper is presented under the UNESCO-IUGS-supported project *IGCP-#475 Deltas in the Monsoon Asia-Pacific Region: DeltaMAP*. Columbia University's work in Araihasar is supported by NIEHS Superfund Basic Research Program grant NIH 1 P42 ES10349 and NSF grant EAR 03-45688

REFERENCES

- Aalto, R., L. Maurice-Bourgoin, T. Dunne, D.R. Montgomery, C.A. Nittrouer, and J.L. Guyot (2003), Episodic sediment accumulation on Amazonian flood plains influenced by El Niño/Southern Oscillation, *Nature*, 425, 493-497.
- Acharyya, S.K., S. Lahiri, B.C. Raymahashay, and A. Bhowmik (2000), Arsenic toxicity of groundwater in parts of the Bengal basin in India and Bangladesh: the role of Quaternary stratigraphy and Holocene sea-level fluctuation, *Environmental Geology*, 39 (10), 1127-1137.

Ahmed, K.M., P. Bhattacharya, M.A. Hasan, S.H. Akhter, S.M. Mahbub Alam, M.A. Hossain Bhuyian, M.B. Imam, A.A. Khan, and O. Sracek (2004), Arsenic enrichment in groundwater of the alluvial aquifers in Bangladesh: an overview, *Applied Geochemistry*, 19, 181-200.

Aziz, Z., A. van Geen, R. Versteeg, A. Horneman, Y. Zheng, S. Goodbred, M. Steckler, M. Stute, B. Weinman, I. Gavrieli, M. Shamsudduha, M.A. Hoque, and K.M. Ahmed (2005), Arsenic concentrations in shallow groundwater of Araihasar, Bangladesh: Part II. Hydrologic control reflected in the electromagnetic conductivity of soils, *Water Resour. Res.*, *this volume*.

Kinniburgh D.G., and P. Smedley, editors (2001), BGS/DPHE reports, arsenic contamination of groundwater in Bangladesh. *Technical Rep. WC/00/19, 4 Vol.*, British Geol. Surv., London, UK.

Berg, M., H.C. Tran, T.C. Nguyen, H.V. Pham, R. Schertenleib, and W. Giger (2001), Arsenic contamination of ground and drinking water in Vietnam: a human health threat, *Environ. Sci. Technol.* 35, 2621-2626.

Brammer, H. (1996), *The Geography of the Soils of Bangladesh*, University Press Limited, Dhaka, Bangladesh.

Bridge, J.S. (1993), The interaction between channel geometry, water flow, sediment transport, and deposition in braided rivers, in *Braided Rivers*, Special Publication No. 75, edited by J.L. Best and C.S. Bristow, pp. 13-71, Geological Society of London, UK.

Bristow, C.S. (1987), Brahmaputra River: Channel migration and deposition, in *Recent developments in fluvial sedimentology*, edited by F.G. Etheridge, R.M. Flores and M.D. Harvey, pp. 63-74, SEPM (Society for Sedimentary Geology).

Bristow, C.S. (1999), Gradual avulsion, river metamorphosis and reworking by underfit streams: a modern example from the Brahmaputra River in Bangladesh and possible ancient example in the Spanish Pyrenees, *Spec. Publs. Int. Ass. Sediment*, 28, 221-230.

Chen-Wuing Liu, Cheng-Shin Jang, and Chung-Min Liao (2004), Evaluation of arsenic contamination potential using indicator kriging in the Yun-Lin aquifer (Taiwan), *Science of The Total Environment*, 321(1-3), 173-188.

Cheng, Z., Y. Zheng, R. Mortlock, and A. van Geen (2004), Rapid multi-element analysis of groundwater by high-resolution inductively coupled plasma mass spectrometry, *Analytical and Bioanalytical Chemistry*, 379(3), 512-518.

Cheng, Z., A. van Geen, A.A. Seddique, and K.M. Ahmed (2005), Limited temporal variability of arsenic concentrations in 20 wells monitored for 3 years in Araihasar, Bangladesh, *Environmental Science & Technology*, 39(13), 4759-4766.

Clifford, H.T. and W. Stephenson (1975), *An Introduction to Numerical Classification*, 229 pp., Academic Press, New York.

Coleman, J.M. (1969), Brahmaputra river: channel processes and sedimentation, *Sedimentary Geology*, 3(2-3), 129-239.

Datta, D.K., and V. Subramanian (1997), Texture and mineralogy of sediments from the Ganges-Brahmaputra-Meghna river system in the Bengal Basin, Bangladesh and their environmental implications, *Environmental Geology*, 30, 181-188.

Fergusson, J. (1863), On Recent changes in the delta of the Ganges, *Quarterly Journal of the Geological Society of London*, 19, 321-354.

Goodbred, S.L., and S.A. Kuehl (1998), Floodplain processes in the Bengal Basin and the storage of Ganges-Brahmaputra sediment: an accretion study using ^{137}Cs and ^{210}Pb geochronology, *Sedimentary Geology*, 121, 239-258.

Goodbred, S.L., and S.A. Kuehl (2000), The significance of large sediment supply, active tectonism, and eustasy on margin sequence development: Late Quaternary stratigraphy and evolution of the Ganges-Brahmaputra delta, *Sedimentary Geology*, 133, 227-248.

He, Q., and E. Walling (1996), Use of fallout Pb-210 measurements to investigate longer-term rates and patterns of overbank sediment deposition on the floodplains of lowland rivers, *Earth Surface Processes and Landforms*, 21, 141-154.

Horneman, A., A. van Geen, D. Kent, P.E. Mathe, Y. Zheng, R.K. Dhar, S. O'Connell, M.Hoque, Z. Aziz, M. Shamsudduha, A. Seddique, and K.M. Ahmed (2004), Decoupling of arsenic and iron release to Bangladesh groundwater under reducing conditions. Part I: Evidence from sediment profiles, *Geochim. Cosmochim. Acta.*, 68(17), 3459-3473.

Ingebritsen, S.E. and W.E. Sanford, (1998), *Groundwater in Geologic Processes*, Cambridge University Press, NY.

Jain, M., S.K. Tandon, S.C. Bhatt, A.K. Singhvi, and S. Mishra (1999), Alluvial and aeolian sequences along the River Luni, Barmer District; physical stratigraphy and feasibility of luminescence chronology methods, in *Memoir*, edited by B.P. Radhakrishna and S.S. Merh, pp. 273-295, Geological Society of India, Vadodara, India.

Kale, V.S., A.K. Singhvi, P.K. Mishra, and D. Banerjee (2000), Sedimentary records and luminescence chronology of late Holocene palaeofloods in the Luni River, Thar Desert, Northwest India, *Catena (Giessen)*, 40(4), 337-358.

Lamy, F., D. Hebbeln, and G. Wefer (1998), Late Quaternary precessional cycles of terrigenous sediment input off the Norte Chico, Chile (27.5°S) and palaeoclimatic implications, *Palaeogeography, Palaeoclimatology, Palaeoecology*, 141(3-4), 233-251.

McArthur, J.M., D.M. Banerjee, K.A. Hudson-Edwards, R. Mishra, R. Purohit, P. Ravenscroft, A. Cronin, R.J. Howarth, A. Chatterjee, T. Talukder, D. Lowry, S. Houghton, and D.K. Chadha

(2004), Natural organic matter in sedimentary basins and its relation to arsenic in anoxic groundwater: the example of West Bengal and its worldwide implications, *Applied Geochemistry*, 19, 1255-1293.

Murray, A.S., and A.G. Wintle (2000), Luminescence dating of quartz using an improved single-aliquot regenerative-dose protocol, *Radiation Measurements*, 32, 57-73.

Nickson, R.T., J.M. McArthur, P. Ravenscroft, W.G. Burgess, and K.M. Ahmed (2000), Mechanism of arsenic release to groundwater, Bangladesh and West Bengal, *Applied Geochemistry*, 15, L403-413.

Prescott, J.R., and J.T. Hutton (1988), Cosmic ray and gamma ray dosimetry for TL and ESR, *Nuclear Tracks and Radiation Measurements*, 14, 223-227.

Rasid, H. (1966), Morphology of the Jamuna flood plains, *The Oriental Geographer*, 10(2), 57-72.

Sengupta, S., P.K. Mukherjee, T. Pal, and S. Shome (2004), Nature and origin of arsenic carriers in shallow aquifer sediments of Bengal Delta, India, *Environmental Geology*, 45, 1071–1081.

Smedley, P.L., M. Zhang, G. Zhang, and Z. Luo (2003), Mobilization of arsenic and other trace metals in fluviolacustrine aquifers of the Huhhot Basin, Inner Mongolia, *Applied Geochemistry*, 18, 1453-1477.

Srivastava, P., N. Juyal, A.K. Singhvi, R.J. Wasson, and M.D. Bateman (2001), Luminescence chronology of river adjustment and incision of Quaternary sediments in the alluvial plain of the Sabarmati River, north Gujarat, India, *Geomorphology*, 36, 217-229.

Stute, M., Y. Zheng, P. Schlosser, A. Horneman, R.K. Dhar, M.A. Hoque, A.A. Seddique, M. Shamsudduha, K.M. Ahmed, and A. van Geen (2005). Increase in arsenic concentrations with groundwater age in shallow Bangladesh aquifers, *Water Resour. Res.*, in submission.

van Geen, A., H. Ahsan, A.H. Horneman, R.K. Dhar, Y. Zheng, I. Hussain, K.M. Ahmed, A. Gelman, M. Stute, H.J. Simpson, S. Wallace, C. Small, F. Parvez, V. Slavkovich, N.J. LoIacono, M. Becker, Z. Cheng, H. Momotaj, M. Shahnewaz, A.A. Seddique, and J.H. Graziano (2002), Promotion of well-switching to mitigate the current arsenic crisis in Bangladesh, *Bulletin of the World Health Organization*, 80, 732-737.

van Geen, A., Y. Zheng, R. Versteeg, M. Stute, A. Horneman, R. Dhar, M. Steckler, A. Gelman, C. Small, H. Ahsan, J. H. Graziano, I. Hussain, and K. M. Ahmed, (2003), Spatial variability of arsenic in 6000 tube wells in a 25 km² area of Bangladesh, *Water Resour. Res.*, 39(5), 1140.

van Geen, A., T. Protus, Z. Cheng, A. Horneman, A.A. Seddique, M.A. Hoque, and M. Ahmed (2004), Testing groundwater for arsenic in Bangladesh before installing a well, *Environmental Science and Technology*, 38(24), 6783-6789.

Yu, W.H., C.M. Harvey, and C.F. Harvey (2003), Arsenic in groundwater in Bangladesh: A geostatistical and epidemiological framework for evaluating health effects and potential remedies, *Water Resources Research*, 39(6), 1146.

Zheng, Y., M. Stute, A. van Geen, I. Gavrieli, R. Dhar, J.H. Simpson, P. Schlosser, and K.M. Ahmed (2004), Redox control of arsenic mobilization in Bangladesh groundwater, *Applied Geochemistry*, 19(2), 201-214.

Zheng, Y., A. van Geen, M. Stute, R. Dhar, Z. Mo, Z. Cheng, A. Horneman, I. Gavrieli, H.J. Simpson, R. Versteeg, M. Steckler, S. Goodbred, K.M. Ahmed, M. Shanewaz, and M. Shamsudduha, (2005), Contrast in groundwater arsenic in shallow Holocene and older deep aquifers: a case study in two villages of Araihasar, Bangladesh, *Geochem. Cosmochem. Acta*, in submission.

FIGURE CAPTIONS

Figure 1. Location of Araihasar study site in the mid-delta portion of Bangladesh. The left panel is a nationwide map showing Araihasar's location between the modern Meghna River to the east and an uplifted Pleistocene Terrace (depicted by a darkening of the surface) to the north and west. The right panel is a closer IKONOS image of Araihasar (van Geen et al., 2003), which shows the complex scrolling topography of this floodplain region.

Figure 2. Four main auger (I-I', II-II', III-III', and IV-IV') and needle-sample (part of III-III' and IV-IV') transects within the arsenic heterogeneous floodplain of Araihasar, Bangladesh. Auger and needle-sample, OSL, and radioisotope locations are denoted by white squares, grey

triangles, and dark grey diamonds, respectively, with the concentration of arsenic in shallow wells depicted in grayscale from 6 to 15m depths (mean concentration of the 101-1000 category is $245 \pm 122 \mu\text{g/L}$). Villages with multiwell locations referred to in the text are depicted using smaller font lettering as MW-A, MW-B, MW-C, MW-F and MW-G. A depth-to-sand interpolated surface is also shown, classified by a natural jenks method that minimizes squared deviations between class means in the data, and indicates a general trend of higher tubewell arsenic coincident to locations where this surface deepens. The Pb-210 and Cs-137 transect is comprised of duplicate samples taken from five locations spanning from the apex of the modern-day meander to a central site in Araihaazar. Samples OSL1 and OSL2 were taken at locations proximal to the modern river, while OSL3 was garnered from a scroll-plain superimposed by the modern-day river.

Figure 3. Ternary diagram depicting the six different sediment facies (i-medium-fine sands, ii-silty-fine sands, iii-mixed silts, iiia-silts, iv-clayey silts, and iva-clays) comprising the floodplain as delineated by cluster analysis of the hydrometer and settling tube data. Interpretations of these facies include iv as fine abandoned channel fill, iii as proximal floodplain deposits, iiia as distal floodplain deposits, ii and iia as bar deposits, and i as channel deposits.

Figure 4, depicting the stratigraphic facies in Araihaazar. In the bottom panel, patterns of thickness and stacking order of the sedimentary facies are shown, comprising the five basic stratigraphies found: pure undiluted sands (strat. facies A), alternating layers of silt and sand (B), mud capped sands (C), fine-grained stratigraphies of silts and clays (D), and the anthropogenic mud capped sands (E). The relative elevations of the sequences are indicated by the offsetting of

the columns, and the sedimentary facies typically amalgamated within the sections are identified with small Roman numerals. The sections are drawn from left to right in order of increasing depth-to-sand, with brackets on the side indicating the thickness of surficial muds for each section. The pictures of the pit walls from OSL sites 1-3 in the top trimerous panel show stratigraphic sections B and C: OSL1 and 3 have the alternating stratigraphy of silts and sands, while OSL2 is a typical mud-capped sand sequence. The unconformable surface between the muds and well sorted sands used for OSL dating are delineated in the photographs by dashed lines. Dates indicated within the photos correspond to the upper few cm of sands buried directly beneath the mud unconformity.

Figures 5a-5d, show how arsenic heterogeneity in the shallow aquifer relates to some of the stratigraphic heterogeneity in Araihasar. Each transect, (I-I', II-II', III-III', and IV-IV') shows the lay of sediments in the top 24m of the aquifer with all sampling points plotted as depth from the DTED elevation surface for a more in-situ depiction of the spatial patterns in existence within the subsurface. Dissolved arsenic concentrations from the shallow tubewells monitored in the 6000 well survey (van Geen, 2003) within 50m of the transects are graphed at an adjusted depth (DTED elevation minus reported well depth) within the stratigraphic cross-sections, with blue circles corresponding to groundwater arsenic concentrations between 0-10 $\mu\text{g/L}$, green circles between 11-50 $\mu\text{g/L}$, yellow between 51-100 $\mu\text{g/L}$, and red circles between 101-1000 $\mu\text{g/L}$.

Figures 6a-f. Graphs showing how depth-to-sand measurements correlate to shallow (<23m) tubewell arsenic measurements from the 6000 well study by van Geen et al. (2002 and 2003).

The depth-to-sand measurements are reported here on the x-axis as minimum (6a,d), mean (6b,e), and maximum (6c,f) values for arsenic concentrations as determined from the depth-to-sand interpolation in Figure 2 using the zonal statistics spatial analyst function of ArcView 8.3. The representations of depth-to-sand vs. arsenic are included as they show how increasing thicknesses of the upper few meters of muds correlate to the concentration of arsenic in the aquifer sands 10-15 meters below. Minimum depth-to-sand values and mud units <4m have more structure in the dataset versus the inclusion of thicker units of overlying mudlayers. The bottom graphs (d, e, and f) exclude data points $\geq 4\text{m}$ and produce a better correlation for arsenic minimum depth-to-sand values. This is likely due to the fact that tube-wells are not typically emplaced in sequences underlying several meters of mud, as indicated by arsenic data offsets in the stratigraphic cross-sections of Figure 5. The decoupling of arsenic from higher depth-to-sand values may also be due to the coinciding nature of more heterogeneous distributions of sediments in villages that anthropogenically modify their elevation.

Figure 7. The geochronology of Araihasar showing that the area is a highly complex geomorphological setting with pleistocene terraces juxtaposed next to channel deposits and abandoned floodplain topography within a km spatial scale.

Figure 8. Model of floodplain evolution and shallow aquifer development, which accounts for some of the heterogeneity of sediments and arsenic in Araihasar. The first stage of the model portrays the region during active river phase <600ya, when the Brahmaputra flowed along its eastern corridor. The second stage of evolution occurred between 400 and 600ya, when the active, high energy system started waning in the region. Finer sedimentation and an initial

phase of infilling began during a 200a series of avulsion and rejuvenation events, ending 200ya at stage 3, when the Brahmaputra switched to its modern course, leaving behind the moribound floodplain we see today.

TABLES

Table 1. Sedimentary Facies

Sedimentary Facies	Lithology	Mean grain size (μm)	Mean Sand:Silt:Clay (%)	Color	Loss-on-Ignition (% wt)	Interpreted Depositional Setting ^a
<i>i</i>	generally well-sorted fine to medium sands	252.1	90:10:0	tan to light gray	<1	channel deposits
<i>ii, ii_a</i>	silty fine sands to clean silts	<i>ii</i> = 73.2 <i>ii_a</i> = 15.2	65:30:5 <i>ii_a</i> (20:75:5)	tan to light gray	<2	bar deposits
<i>iii, iii_a</i>	poorly sorted, sandy muds to clayey silts	<i>iii</i> = 23.5 <i>iii_a</i> = 11.5	25:50:25 <i>iii_a</i> (0:50:50)	yellow-brown to brown	2-5	overbank (floodplain) deposits
<i>iv</i>	silty clays	3.9	10:60:30	brown to dark gray	5-20	abandoned channel fill

^aNOTE: Sediments have been grouped here based on their major environmental association, but the grain-size distributions reveal a continuum of sediment types and facies are not meant to be exclusive categories

Table 2. Stratigraphic Facies

Facies	Stratigraphic Sequence	Surface Elevation	Thickness of mud cap	Associated sediment facies of mud cap	Distribution in Study Area	Geomorphic Interpretation
<i>A</i>	generally clean bedded sands near surface, coarsening and becoming massive with depth	8-13 m	0-0.2 m	n/a, <i>ii</i>	widespread as curvilinear features (100s m wide x 1000s m long), often sites of village settlements	channel levee or channel bar sequence
<i>B</i>	alternating sand and mud layers near surface, underlain by clean sands	5-12 m	interbedded to 0.5-2 m depth	<i>ii, ii_a, iii</i>	relatively local along edges of facies <i>A</i> and transitions to facies <i>C</i> , often cultivated with vegetable crops	lateral bar sequence
<i>C</i>	silt-dominated muds with minor interlayers of sand and clay near surface, underlain by clean sands	6-11 m	0.5-2.5 m	<i>iii, iii_a</i>	broad, widespread coverage, commonly associated with wheat or rice cultivation (e.g., proximal or distal settings, respectively)	proximal to distal floodplain sequence
<i>D</i>	thick clay-rich muds with minor interlayers of sand and silt, from near surface to depth	6-9 m	3-9 m	<i>iii_a, iv_a</i>	localized in four main areas, often as curvilinear or oblate depressions (10s m wide x 100s m long)	abandoned channel system
<i>E</i>	variable, but mostly muddy deposits; disturbed and redistributed; underlain by clean sands	8-13 m	1-5 m	redistributed <i>ii, ii_a, iii, iv</i>	widespread in certain villages, particularly those near modern streams or where natural elevations are low and subject to flooding	anthropogenic fill, usually deposited over levee/bar sequences (facies <i>A, B</i>)

Table 3
OSL summary of results

Sample	Depth (cm)	U (ppm)	Th (ppm)	K (%)	No. of aliquot	De (Gy, 10%)	Water (%)	Dose rate (Gy/ka)	Age (ka)	De (wtd. Mean)	Age (ka)
Osl #1	35	5.9±1.1	11.6±5.9	2.0±0.1	30	1.60±0.04	20±5	3.4±0.4	0.4±0.1	1.9 ± 0.1	0.5 ± 0.1
Osl #1	65	5.5±0.6	24.1±6.7	2.0±0.1	22	2.0±0.1	20±5	4.0±0.5	0.5±0.1	2.7 ±0.2	0.6 ± 0.1
Osl #2	100	11.6±1.3	15.5±11.3	1.9±0.1	30	3.01±0.03	20±5	4.0±0.7	0.6±0.1	3.7 ± 0.1	0.8 ± 0.1
Osl #3	109	4.9±1.3	9.5±4.5	1.9±0.1	30	3.10±0.08	20±5	3.0±0.5	1.0±0.1	5.0 ± 0.1	1.6 ± 0.2

Table 4
Accretion rates based on OSL data

OSL Site	cm	yr	cm/yr
1	35	400	0.088
1	65	600	0.11
1-middle	30	200	0.15
2	100	500	0.200
3	109	1000	0.109
Avg			0.13
SD			0.04

Table 5
Accretion rates based on ^{210}Pb and ^{137}Cs inventories

Sample	^{210}Pb dpm/cm ²	^{137}Cs dpm/cm ²	R _{Pb} cm/yr	R _{Cs} cm/yr
Pb-1A	43	9	0.07	0
Pb-1B	41	16	0.05	0.12
Pb-2A	68	6	0.16	0
Pb-2B	33	8	0.02	0
Pb-3A	64	5	0.14	0
Pb-3B	46	17	0.07	0.15
Pb-4A	10	18	0	0.17
Pb-4B	0	17	0	0.14
Pb-5A	0	5	0	0
Pb-5B	15	0	0	0
Avg			0.05	0.06
SD			0.06	0.08

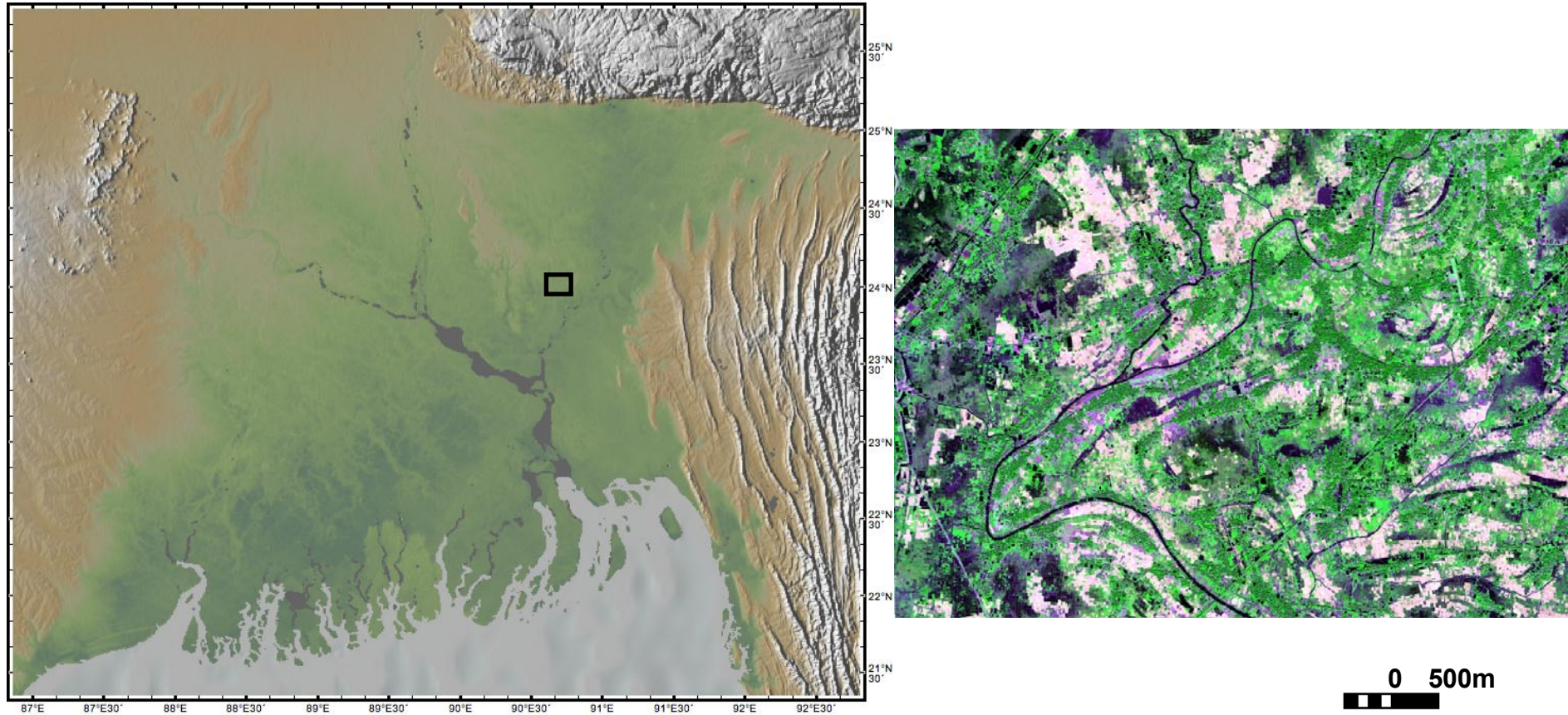


Figure 1. Location of Araihasar study site in the mid-delta portion of Bangladesh. The left panel is a nationwide map showing Araihasar's location between the modern Meghna River to the east and an uplifted Pleistocene Terrace (depicted by a darkening of the surface) to the north and west. The right panel is a closer IKONOS image of Araihasar, which shows the complex scrolling topography of this floodplain region.

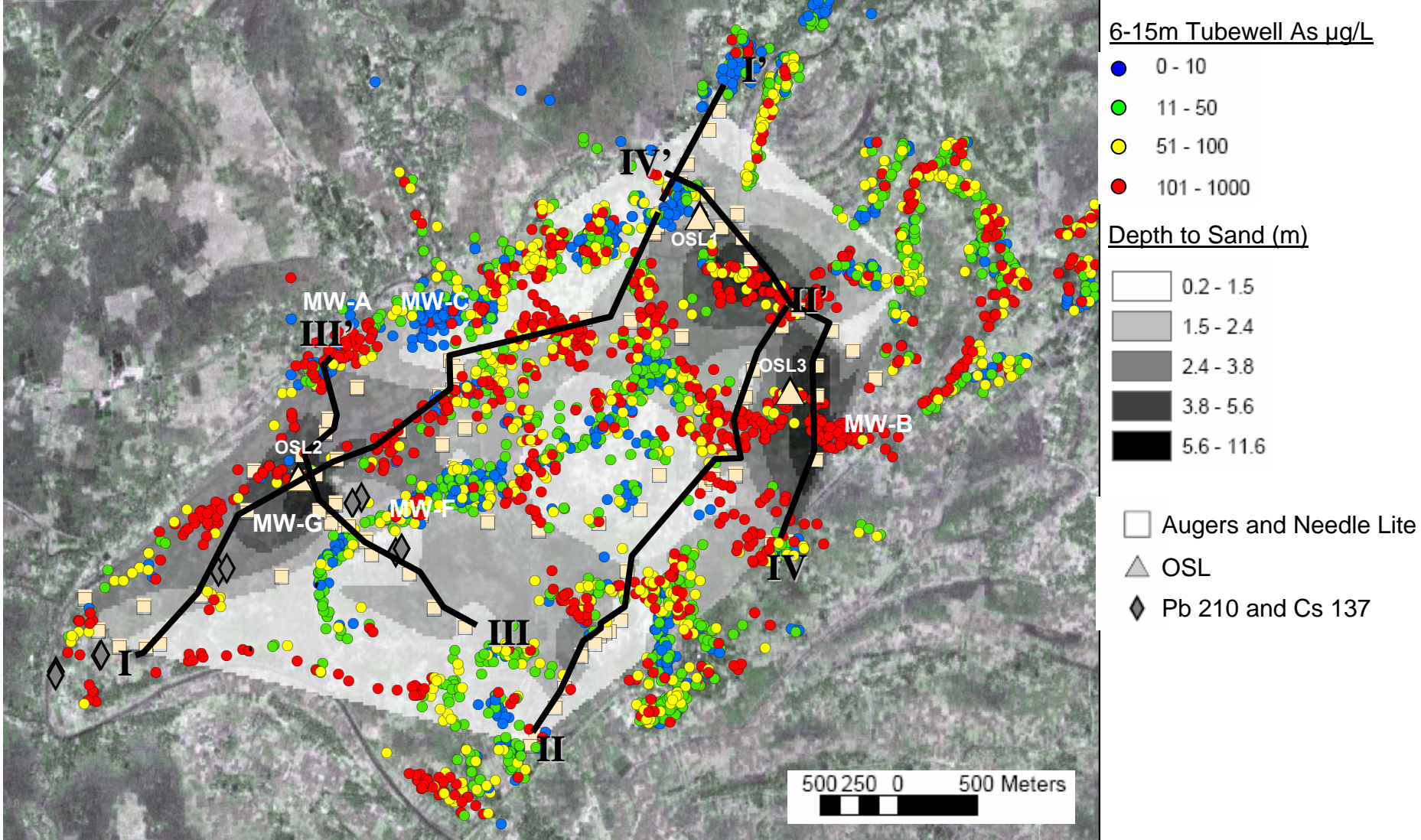


Figure 2. Four main auger (I-I', II-II', III-III', and IV-IV') and needle-sample (part of III-III' and IV-IV') transects within the arsenic heterogeneous floodplain of Araihasar, Bangladesh. Auger and needle-sample, OSL, and radioisotope locations are denoted by white squares, grey triangles, and dark grey diamonds, respectively, with the concentration of arsenic in shallow wells depicted in grayscale from 6 to 15m depths (mean concentration of the 101-1000 category is $245 \pm 122 \mu\text{g/L}$). Villages with multi-iwell locations referred to in the text are depicted using smaller font lettering as MW-A, MW-B, MW-C, MW-F and MW-G. A depth-to-sand interpolated surface is also shown, classified by a natural Jenks method that minimizes squared deviations between class means in the data, and indicates a general trend of higher tube-well arsenic coincident to locations where this surface deepens. The Pb-210 and Cs-137 transect is comprised of duplicate samples taken from five locations spanning from the apex of the modern-day meander to a central site in Araihasar. Samples OSL1 and OSL2 were taken at locations proximal to the modern river, while OSL3 was garnered from a scroll-plain superimposed by the modern-day river.

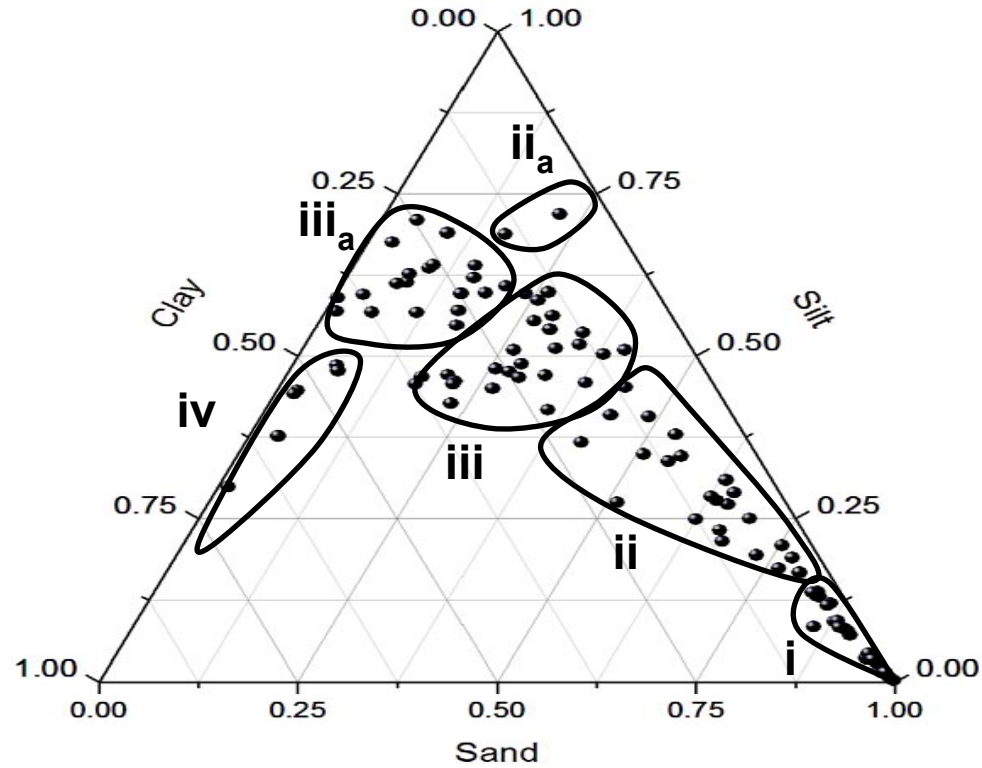


Figure 3. Ternary diagram depicting the six different sediment facies (i-medium-fine sands, ii-silty-fine sands, iii-mixed silts, iii_a-silts, iv-clayey silts, and iv_a-clays) comprising the floodplain as delineated by cluster analysis of the hydrometer and settling tube data. Interpretations of these facies include iv as fine abandoned channel fill, iii as proximal floodplain deposits, iii_a as distal floodplain deposits, ii and ii_a as bar deposits, and i as channel deposits.

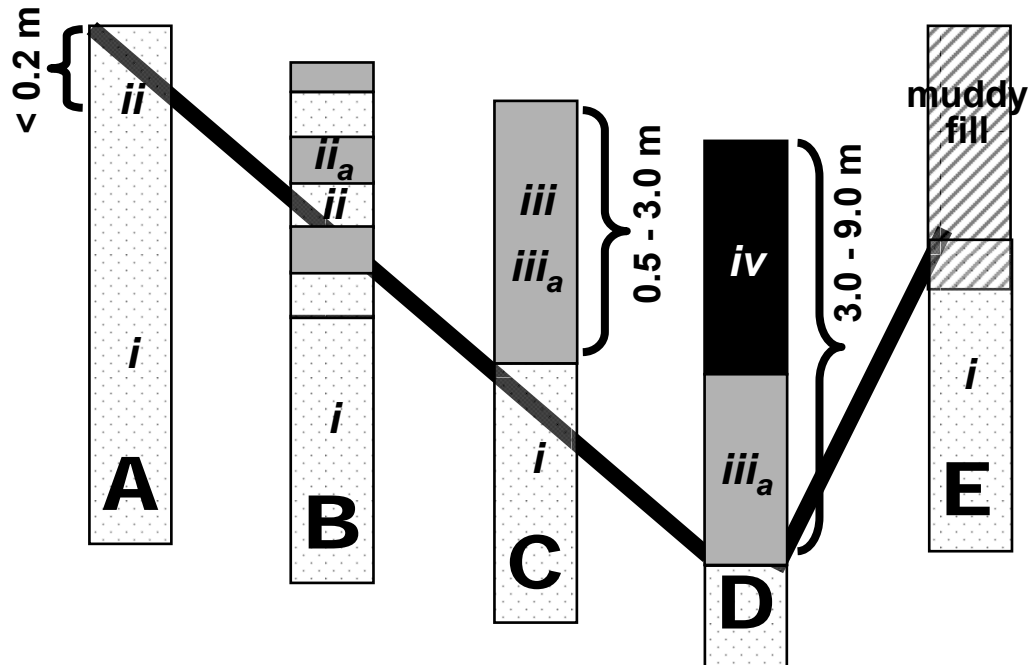
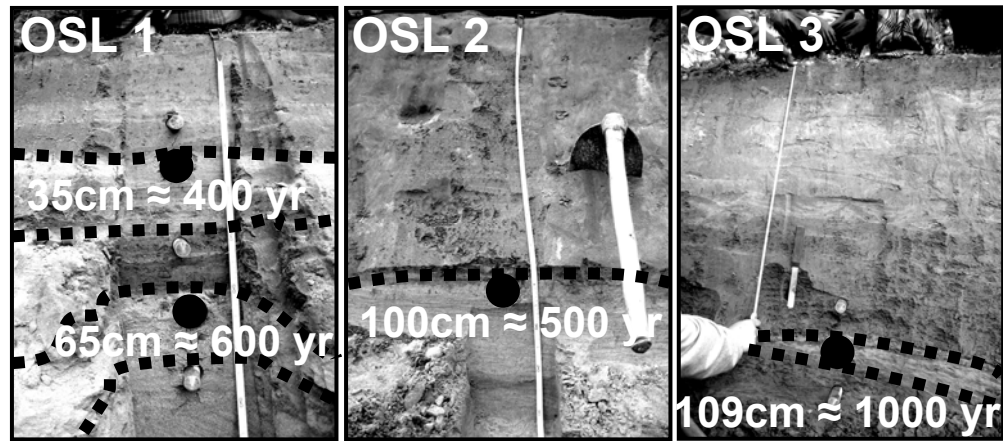
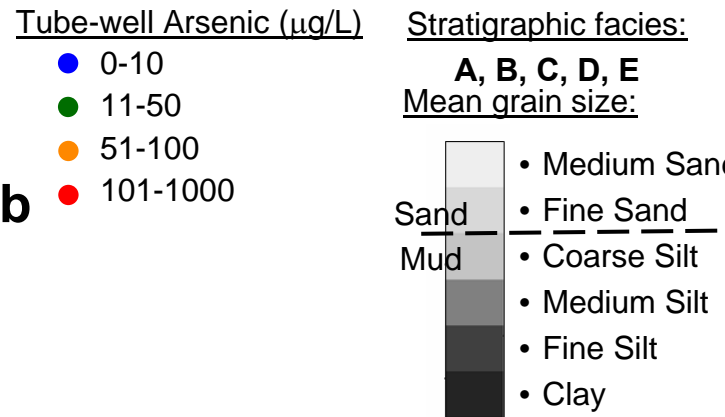
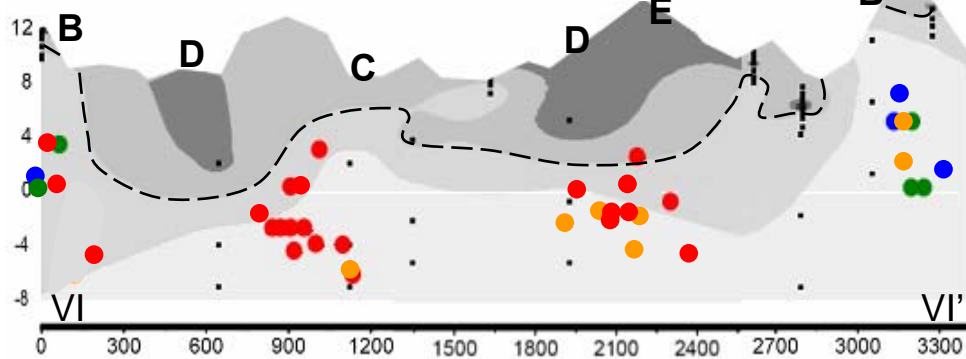
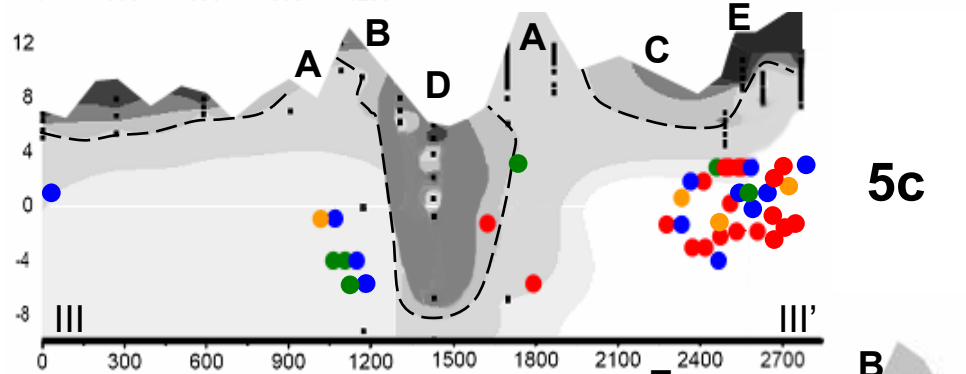
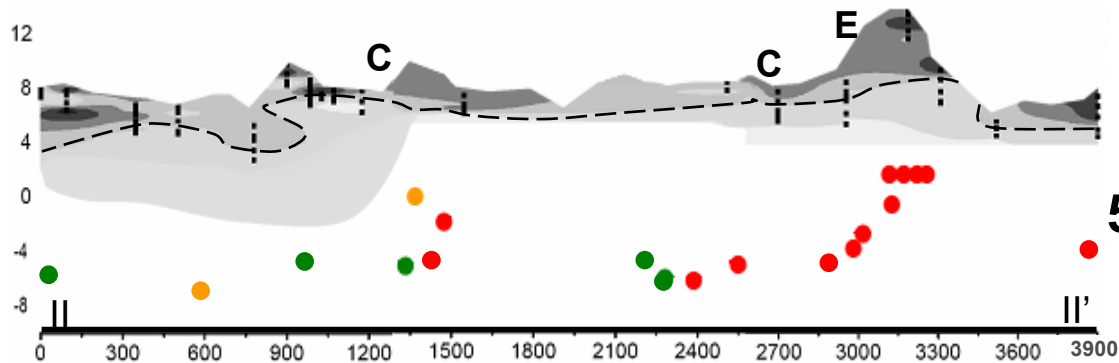
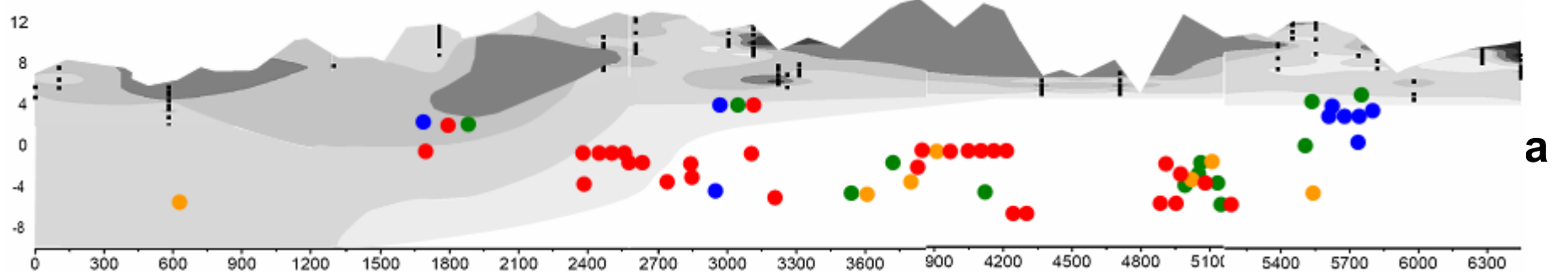
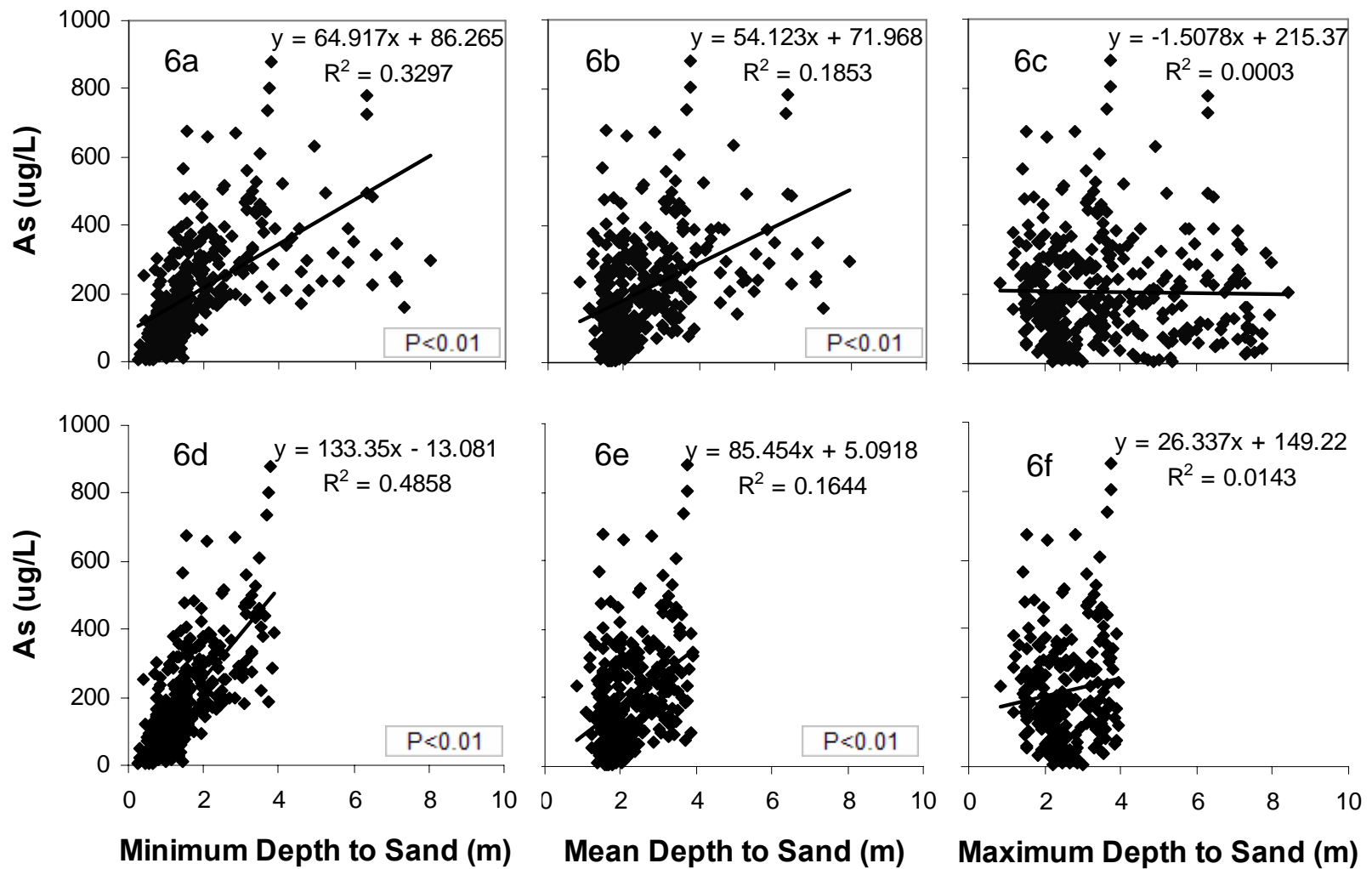


Figure 4, depicting the stratigraphic facies in Arai hazar. In the bottom panel, patterns of thickness and stacking order of the sedimentary facies are shown, comprising the five basic stratigraphies found: pure undiluted sands (strat. facies A), alternating layers of silt and sand (B), mud capped sands (C), fine-grained stratigraphies of silts and clays (D), and the anthropogenic mud capped sands (E). The relative elevations of the sequences are indicated by the offsetting of the columns, and the sedimentary facies typically amalgamated within the sections are identified with small Roman numerals. The sections are drawn from left to right in order of increasing depth-to-sand, with brackets on the side indicating the thickness of surficial muds for each section. The pictures of the pit walls from OSL sites 1-3 in the top trimerous panel show stratigraphic sections B and C: OSL1 and 3 have the alternating stratigraphy of silts and sands, while OSL2 is a typical mud-capped sand sequence. The unconformable surface between the muds and well sorted sands used for OSL dating are delineated in the photographs by dashed lines. Dates indicated within the photos correspond to the upper few cm of sands buried directly beneath the mud unconformity.



Figures 5a-5d, show how arsenic heterogeneity in the shallow aquifer relates to some of the stratigraphic heterogeneity in Araihaazar. Each transect, (I-I', II-II', III-III', and IV-IV') shows the lay of sediments in the top 24m of the aquifer with all sampling points plotted as depth from the DTED elevation surface for a more in-situ depiction of the spatial patterns in existence within the subsurface. Dissolved arsenic concentrations from the shallow tube-wells monitored in the 6000 well survey (van Geen, 2003) within 50m of the transects are graphed at an adjusted depth (DTED elevation minus reported well depth) within the stratigraphic cross-sections, with blue circles corresponding to groundwater arsenic concentrations between 0-10 $\mu\text{g/L}$, green circles between 11-50 $\mu\text{g/L}$, yellow between 51-100 $\mu\text{g/L}$, and red circles between 101-1000 $\mu\text{g/L}$.



Figures 6a-f. Graphs showing how depth-to-sand measurements correlate to shallow (<23m) tube-well arsenic measurements from the 6000 well study by van Geen et al. (2002 and 2003). The depth-to-sand measurements are reported here on the x-axis as minimum (6a,d), mean (6b,e), and maximum (6c,f) values for arsenic concentrations as determined from the depth-to-sand interpolation in Figure 2 using the zonal statistics spatial analyst function of ArcView 8.3. The representations of depth-to-sand vs. arsenic are included as they show how increasing thicknesses of the upper few meters of muds correlate to the concentration of arsenic in the aquifer sands 10-15 meters below. Minimum depth-to-sand values and mud units <4m have more structure in the dataset versus the inclusion of thicker units of overlying mudlayers. The bottom graphs (d, e, and f) exclude data points ≥ 4 m and produce a better correlation for arsenic minimum depth-to-sand values. This is likely due to the fact that tube-wells are not typically emplaced in sequences underlying several meters of mud, as indicated by arsenic data offsets in the stratigraphic cross-sections of Figure 5. The decoupling of arsenic from higher depth-to-sand values may also be due to the coinciding nature of more heterogeneous distributions of sediments in villages that anthropogenically modify their elevation.

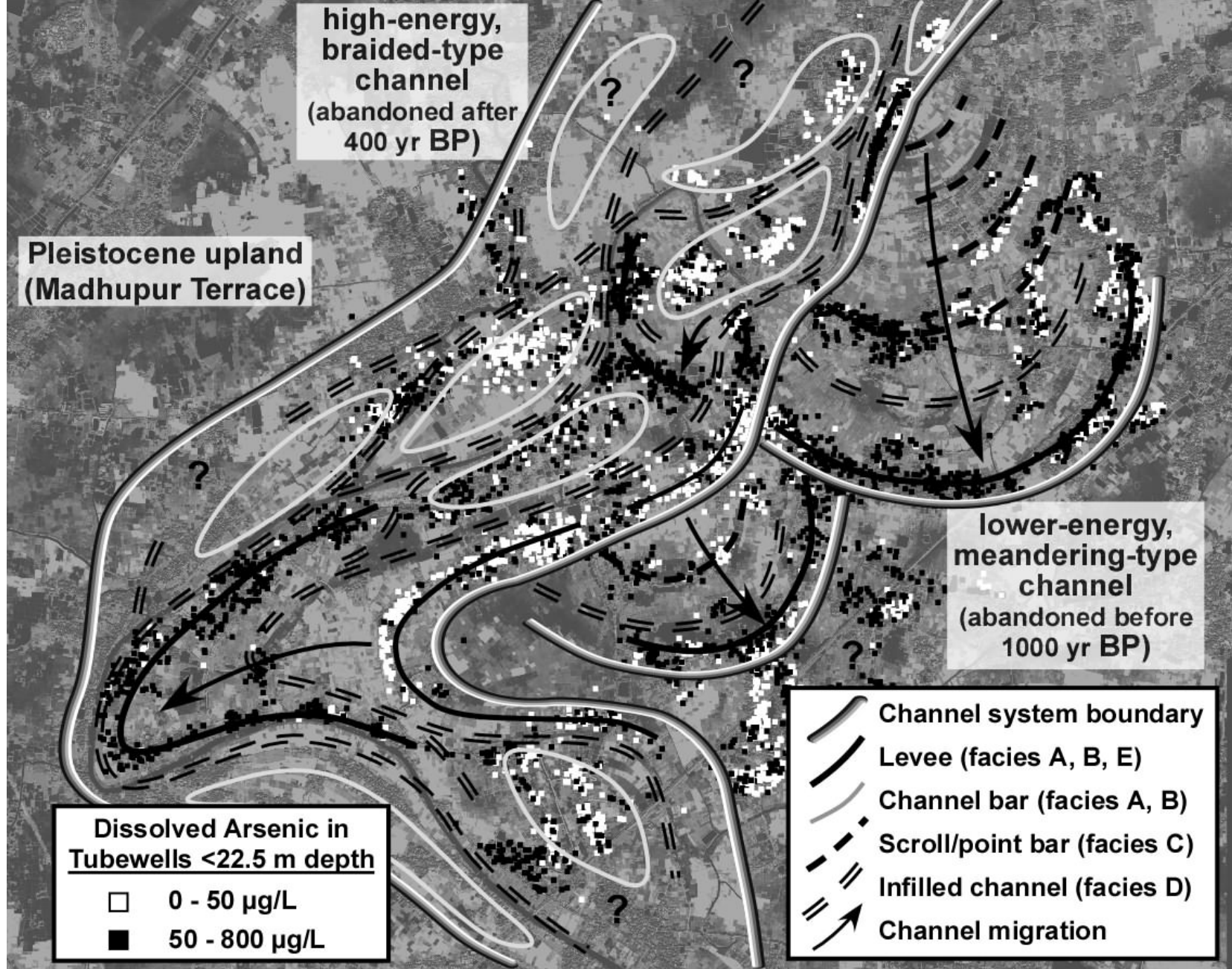
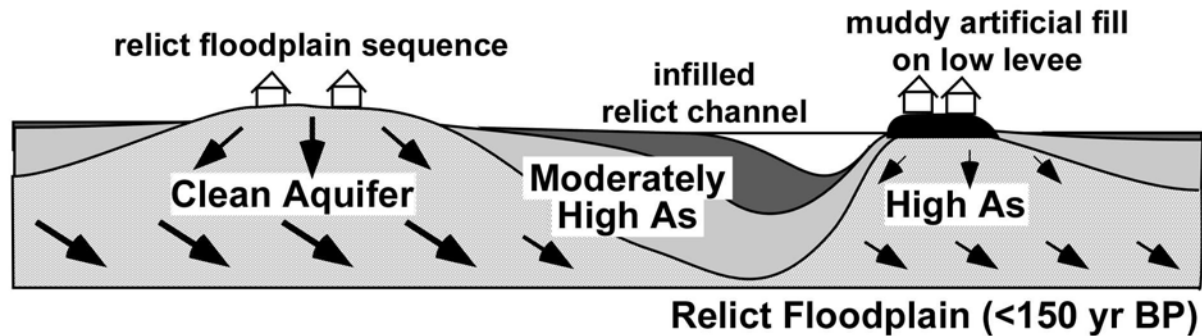
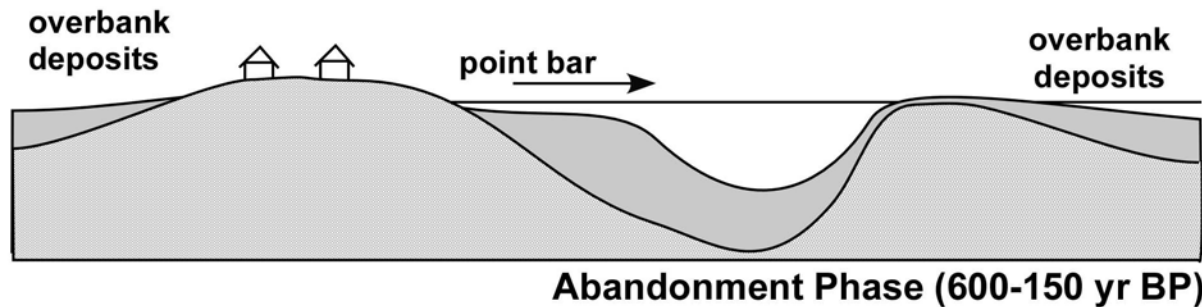
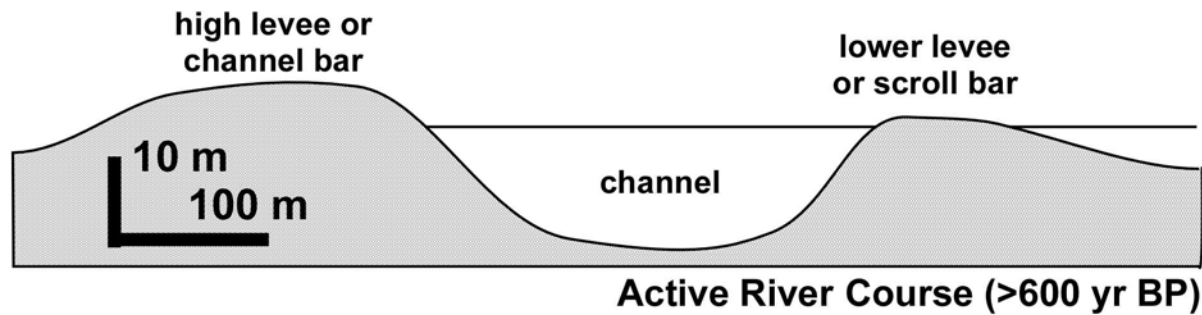


Figure 7. The geochronology of Araihaazar showing that the area is a highly complex geomorphological setting with Pleistocene terraces juxtaposed next to channel deposits and abandoned floodplain topography within a km spatial scale.



Net Groundwater Flow



Sedimentary Facies

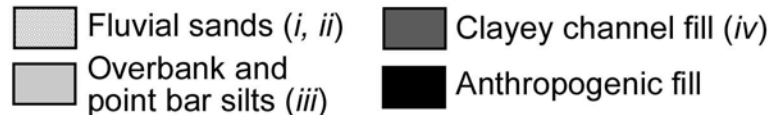


Figure 8. Model of floodplain evolution and shallow aquifer development, which accounts for some of the heterogeneity of sediments and arsenic in Araihaazar. The first stage of the model portrays the region during active river phase <600ya, when the Brahmaputra flowed along its eastern corridor. The second stage of evolution occurred between 400 and 600ya, when the active, high energy system started waning in the region. Finer sedimentation and an initial phase of infilling began during a 200a series of avulsion and rejuvenation events, ending 200ya at stage 3, when the Brahmaputra switched to its modern course, leaving behind the moribund floodplain we see today.